PROCEEDINGS OF SCIENCE

Recent Progress of Light-Front Quark Model Phenomenology

Chueng-Ryong Ji*
Department of Physics, North Carolina State University, Raleigh, NC 27695-8202, USA
E-mail: ji@ncsu.edu

Ho-Meoyng Choi
Department of Physics, Teachers College, Kyungpook National University, Daegu, Korea 702-701
E-mail: homyoung@knu.ac.kr

Martin DeWitt
Department of Chemistry and Physical Sciences, High Point University, High Point, NC 27262, USA
E-mail: mdewitt@highpoint.edu

We discuss recent progress of light-front quark model (LFQM) phenomenology. In particular, we present the scalar glueball candidate from the LFQM analysis and the consistency of our result with the chiral suppression of the scalar glueball decay to a pair of quark and antiquark. Our LFQM also supports the recent findings from the AdS/QCD correspondence checking the dispersion relation for the timelike pion form factor.

LIGHT CONE 2008 Relativistic Nuclear and Particle Physics
July 7-11 2008
Mulhouse, France

*Speaker.

PoS(LC2008)023

1. Introduction

Various hadron-related experimental measurements such as generalized parton distributions and single spin asymmetries at JLab and DESY (Hermes), B-decays at SLAC (BABAR) and KEK (Belle) as well as quark gluon plasma production at BNL (RHIC) and CERN (ALICE), etc. may be provided in a unified framework of light-front dynamics (LFD). Owing to the rational energy-momentum dispersion relation, LFD has distinct features compared to other forms of Hamiltonian dynamics. In particular, the vacuum fluctuations are suppressed and the kinematic generators are proliferated in LFD. Overall, these distinct features can be regarded as advantageous in hadron phenomenology. However, it has also been emphasized that treacherous points such as zero-mode contributions should be taken into account for successful LFD applications to hadron phenomenology.

In this paper, we discuss some recent progress of light-front quark model (LFQM) phenomenology. In particular, we present a new development in scalar meson spectroscopy and their hadronic decays and comment on the connection between the AdS/QCD approach and the usual LF formalism for hadronic form factors. Firstly, the structure of the scalar mesons has long been an enigma in hadron spectroscopy. Unlike the elegant vector and tensor multiplets, it is still controversial which are the members of the expected $L = S = 1$ $q\overline{q}$ multiplet since there are now too many 0^{++} mesons observed in the region below 2 GeV for them all to be explained naturally within a $q\overline{q}$ picture [1]. This has led to the suggestion that not all of them are $q\overline{q}$ states. The main reason for this situation is that around the relevant mass region there exist other structures such as $K\overline{K}$ molecules [2], glueballs [3], and four-quark ($qq\overline{qq}$) systems [4]. In an attempt to decipher the structure of these states, we investigate a scenario in which $f_0(1370)$, $f_0(1500)$, and $f_0(1710)$ are admixtures of quarkonia and the lowest–lying scalar glueball. The spectrum is computed using a relativized, QCD-inspired model Hamiltonian. The results of the spectrum calculation are used to analyze the mixing between the $q\overline{q}$ and glueball. Our final result indicates that $f_0(1710)$ is dominantly composed of the scalar glueball, while $f_0(1370)$ and $f_0(1500)$ are mainly $n\overline{n}$–$s\overline{s}$ mixtures. Secondly, using the connection between the AdS/QCD and the LF approaches in the calculation of the hadronic form factors [5], we calculated [6] the pion form factor in our LFQM taking into account a momentum-dependent dynamical quark mass. We confirmed that the power-law behavior of the pion form factor is indeed attained by taking into account a momentum-dependent dynamical quark mass which becomes negligible at large momentum region. Our result [6] was consistent with an important point of AdS/QCD prediction, namely, the holographic wave function contains the contribution from all scales up to the confining scale. Finally, we went beyond the peaking approximation for the calculation of the exclusive $J/\psi + \eta_c$ production in e^+e^- annihilation process to reduce the discrepancy between the theoretical predictions based on the NRQCD factorization approach and the experimental results [7]. Our work on the double charm production process is presented in a separated contribution to this conference proceedings [8].

The paper is organized as follows. In Sec. 2, we describe the formulation of our LFQM and present our analysis of the glueball candidate in the scalar meson spectroscopy. In Sec.3, we discuss the recent development of AdS/QCD approach and the support from the LFQM with the investigation on the dispersion relation for the timelike pion form factor. Summary and conclusions follow in Sec.4.

PoS(LC2008)023

2. LFQM and Meson Spectroscopy

The key idea in our LFQM [9] for mesons is to treat the radial wave function as trial function for the variational principle to the QCD-motivated effective Hamiltonian saturating the Fock state expansion by the constituent quark and antiquark. The QCD-motivated Hamiltonian for a description of the ground state meson mass spectra is given by

$$H_{q\bar{q}}|\Psi^{JJ_z}_{nlm}\rangle = \left[\sqrt{m_q^2+\vec{k}^2}+\sqrt{m_{\bar{q}}^2+\vec{k}^2}+V_{q\bar{q}}\right]|\Psi^{JJ_z}_{nlm}\rangle = M_{q\bar{q}}|\Psi^{JJ_z}_{nlm}\rangle, \tag{2.1}$$

where $\vec{k}=(\mathbf{k}_\perp,k_z)$ is the three-momentum of the constituent quark, $M_{q\bar{q}}$ is the mass of the meson, and $|\Psi^{JJ_z}_{nlm}\rangle$ is the meson wave function. We use two interaction potentials $V_{q\bar{q}}$ for the pseudoscalar (0^{-+}) and vector (1^{--}) mesons: (1) Coulomb plus harmonic oscillator (HO), and (2) Coulomb plus linear confining potentials. In addition, the hyperfine interaction, which is essential to distinguish vector from pseudoscalar mesons, is included for both cases, viz.,

$$V_{q\bar{q}} = V_0 + V_{\text{hyp}} = a + \mathscr{V}_{\text{conf}} - \frac{4\alpha_s}{3r} + \frac{2}{3}\frac{\mathbf{S}_q\cdot\mathbf{S}_{\bar{q}}}{m_q m_{\bar{q}}}\nabla^2 V_{\text{coul}}, \tag{2.2}$$

where $\mathscr{V}_{\text{conf}} = br(r^2)$ for the linear (HO) potential. The momentum space LF wave function of the ground state pseudoscalar and vector mesons is given by $\Psi(x_i,\mathbf{k}_{i\perp},\lambda_i)=\mathscr{R}_{\lambda_1\lambda_2}(x_i,\mathbf{k}_{i\perp})\phi_R(x_i,\mathbf{k}_{i\perp})$, where $\phi_R(x_i,\mathbf{k}_{i\perp})$ and $\mathscr{R}_{\lambda_1\lambda_2}$ are the radial- and the spin-orbit wave functions, respectively. For the radial wave function ϕ_R, we use the same Gaussian wave function for both pseudoscalar and vector mesons $\phi_R(x_i,\mathbf{k}_{i\perp})=(4\pi^{3/4}/\beta^{3/2})\sqrt{\partial k_z/\partial x}\exp(-\vec{k}^2/2\beta^2)$, where β is the variational parameter and $\partial k_z/\partial x = M_0/(4x_1x_2)$ the Jacobian of the variable transformation $\{x,\mathbf{k}_\perp\}\to k=(\mathbf{k}_\perp,k_z)$. The spin-orbit wave functions for both pseudoscalar and vector mesons satisfy $\sum_{\lambda_1\lambda_2}\mathscr{R}^\dagger_{\lambda_1\lambda_2}\mathscr{R}_{\lambda_1\lambda_2}=1$. For the scalar ($^3P_0$) mesons possessing non-zero orbital angular momentum [10], we use $\phi_R^{(S)}(x_i,\mathbf{k}_{i\perp})$ $=\sqrt{2/3\beta^2}\phi_R(x_i,\mathbf{k}_{i\perp})$ and the spin-orbit wave function for $^3P_0$ state satisfies $\sum_{\lambda_1\lambda_2}\mathscr{R}^{S\dagger}_{\lambda_1\lambda_2}\mathscr{R}^S_{\lambda_1\lambda_2}=$ $|\vec{k}^2|$.

For the pseudoscalar and vector meson mass spectra, we apply our variational principle to the QCD-motivated effective Hamiltonian first to evaluate the expectation value of the central Hamiltonian, i.e. $\langle\phi_R|(H_0+V_0)|\phi_R\rangle$ with a trial function $\phi_R(x_i,\mathbf{k}_{i\perp})$ that depends on the variational parameters β with β being varied until $\langle\phi_R|(H_0+V_0)|\phi_R\rangle$ is a minimum. Once these model parameters are fixed, then, the mass eigenvalue of each meson is obtained as $M_{q\bar{q}}=\langle\phi_R|(H_0+V_{q\bar{q}})|\phi_R\rangle$. More detailed procedure of determining the model parameters of light and heavy quark sectors can be found in our previous works [9]. Our predictions obtained from both the linear and the HO parameters are overall in good agreement with the data within 6% error.

For the scalar meson case, we compute the spectrum using the relativized, QCD-inspired model Hamiltonian of Godfrey and Isgur [11]. Since the scalar mesons possess non-zero orbital angular momentum, the Hamiltonian includes spin–orbit interactions as well as the spin–spin interactions and linear confining potential used in previous pseudoscalar and vector meson analyses. The potentials are relativized by first smearing out the position coordinate over distances on the order of the inverse quark masses, and secondly by replacing the quark masses with the quark energies. The latter correction makes the potentials dependent on the momenta of the interacting quarks. The relativized Hamiltonian is diagonalized using a basis of 25 simple harmonic oscillator states. For details about the Hamiltonian and the resulting spectrum see Ref. [12].

The masses and wave functions from the spectrum calculation are then used to analyze the mixing of the scalar mesons. We adopt a scheme in which the conventional scalar $q\bar{q}$ states and the lowest–lying scalar glueball (gg) mix to produce to the three isoscalar states $f_0(1370)$, $f_0(1500)$, and $f_0(1710)$.

$$\begin{pmatrix} |f_0(1370)\rangle \\ |f_0(1500)\rangle \\ |f_0(1710)\rangle \end{pmatrix} = U \begin{pmatrix} |n\bar{n}\rangle \\ |s\bar{s}\rangle \\ |gg\rangle \end{pmatrix} \equiv \begin{pmatrix} a_1 & b_1 & c_1 \\ a_2 & b_2 & c_2 \\ a_3 & b_3 & c_3 \end{pmatrix} \begin{pmatrix} |n\bar{n}\rangle \\ |s\bar{s}\rangle \\ |gg\rangle \end{pmatrix} \tag{2.3}$$

Unlike many other scalar meson mixing analyses, we do not assume glueball dominance. That is, we do not assume that the $q\bar{q}$–$q\bar{q}$ mixing is negligible compared to $q\bar{q}$–gg mixing, but leave the mixing scheme as general as possible. Once the mixing parameters are fixed, the $q\bar{q}$-glue content is used to investigate hadronic decays of the scalar mesons. In particular, we compute the widths for scalar mesons decaying to pairs of pseudoscalar mesons: $f_0 \to \pi\pi$, $f_0 \to K\bar{K}$, and $f_0 \to \eta\eta$. For the decay calculations, two different scenarios are explored. In the first, the contribution of the glueball to the hadronic decays is neglected. In the second scenario, the contributions of the glueball to these decays is included by parameterizing them and fitting these parameters to the decay data.

When the contributions of the glueball to the hadronic decays are neglected, no solution can be found which matches the data. However, when the glueball contributions are included, a very good match to the data is achieved (see [12]). In our best solution,

$$U = \begin{pmatrix} 0.617 & -0.782 & -0.088 \\ 0.676 & 0.581 & -0.453 \\ 0.403 & 0.224 & 0.887 \end{pmatrix}, \tag{2.4}$$

the $f_0(1710)$ is composed mainly of the scalar glueball, while the $f_0(1370)$ and $f_0(1500)$ are dominantly $n\bar{n}$–$s\bar{s}$ mixtures. In addition, the solution requires that the amplitude for $gg \to \pi\pi$ be negligible, while the amplitude for $gg \to K\bar{K}$ is relatively large, and the amplitude for $gg \to \eta\eta$ is even larger. One might expect that the relative sizes of the contributions would be in the reverse order where the pion contribution is largest and the eta meson contribution is smallest due to phase space differences. However, there are reasons to believe that this ordering makes sense.

Sexton, Vaccarino, and Weingarten have published lattice results [13] in which they computed the partial decay widths for the scalar glueball to pairs of pseudoscalar mesons in the quenched approximation. They found that the coupling increased with increasing pseudoscalar meson mass, so that the decay width to $K\bar{K}$ was larger than the decay width to $\pi\pi$. Additionally, Chanowitz [14] finds that the coupling of a spin zero glueball to light $q\bar{q}$ pairs is chirally suppressed by a factor of m_q/m_{gg}. This is because for $m_q = 0$, chiral symmetry requires the quark and antiquark to have equal chirality, hence unequal helicity, implying non–vanishing net angular momentum, so that the amplitude must vanish for $J = 0$ in the chiral limit. Since the coupling is proportional to the quark mass, this suppression will be stronger for $u\bar{u}$ and $d\bar{d}$ than for $s\bar{s}$. So the glueball could have a significant contribution to $K\bar{K}$ decays, while its contribution to $\pi\pi$ would be small. The $f_0(1710)$ decays more strongly to $K\bar{K}$ than to $\pi\pi$, and this has been taken as evidence that it is mainly an $s\bar{s}$

state. However, if Chanowitz is correct one could interpret the $f_0(1710)$ as being the scalar glueball with its comparatively large $K\bar{K}$ width explained by chiral suppression. This interpretation matches our finding that the $f_0(1710)$ is dominantly composed of the scalar glueball.

3. Timelike Pion Form Factor in Conformal Symmetry

The AdS/QCD correspondence is particularly relevant for the description of hadronic form factors and also provides a convenient framework for analytically continuing the spacelike results to the timelike region. The pion electromagnetic form factor has been exemplified by AdS/QCD, in particular, the power-law behavior of the form factor $F_\pi(Q^2) \sim 1/Q^2$ is well reproduced by the soft-wall AdS/QCD model (or Gaussian model) [15]. The key ingredient in this correspondence is the conformal symmetry valid in the negligible quark mass. Using the connection between the AdS/QCD and the light-front approaches in the calculation of the hadronic form factors, we calculated [6] the pion form factor in our LFQM taking into account a momentum-dependent dynamical quark mass. In particular, we show that the timelike form factor obtained by the analytic continuation of the spacelike form factor correctly satisfies the dispersion relation, $F(q^2) = \mathrm{Re}F(q^2) + i\mathrm{Im}F(q^2)$.

The elastic pion form factor related to pion electromagnetic current by $\langle P'|J^\mu(0)|P\rangle = (P'+P)^\mu F_\pi(Q^2)$ can written as

$$F_\pi(Q^2) = \int_0^1 dx \int d^2\mathbf{k}_\perp \sqrt{\frac{\partial k_z}{\partial x}}\phi_R(x,\mathbf{k}_\perp)\sqrt{\frac{\partial k'_z}{\partial x}}\phi_R(x,\mathbf{k'}_\perp)\frac{m^2+\mathbf{k}_\perp\cdot\mathbf{k'}_\perp}{\sqrt{m^2+\mathbf{k}^2_\perp}\sqrt{m^2+\mathbf{k'}^2_\perp}}, \qquad (3.1)$$

where $\mathbf{k'}_\perp = \mathbf{k}_\perp + (1-x)\mathbf{q}_\perp$ and our calculation was carried out using the q^+=q^0+q^3=0 frame where $q^2 = -Q^2$, i.e. $Q^2 > 0$ is the spacelike momentum transfer. One should understand m as a function of Q^2 in principle although in practice $m(Q^2)$ for the low Q^2 phenomenology can be taken as a constant constituent quark mass. We took the simple parametrization of the quark mass evolution $m(Q^2)$ in spacelike momentum region as $m(Q^2) = m_0 + (m_c - m_0)(1+e^{-0.2})/[1+e^{(Q^2-0.2)}]$, where $m_0 = 5$ MeV and $m_c = 220$ MeV represent the current (at high Q^2) and constituent (at low Q^2) quark mass, respectively [6].

We note that $\phi_R(x,\mathbf{k}_\perp)\phi_R(x,\mathbf{k'}_\perp)$ in Eq. (3.1) provides a mass-dependent weighting factor $e^{-\frac{m^2}{4x(1-x)\beta^2}}$ which severely suppresses the contribution from the endpoint region of $x \to 0$ and 1 unless $m \to 0$. This weighting factor leads to the gaussian fall-off of $F_\pi(Q^2)$ at high Q^2 region for the constant constituent quark mass which breaks the conformal symmetry. When the conformal symmetry limit ($m \to 0$) is taken, however, there is no such suppression of the endpoint region and the high Q^2 behavior of the form factor dramatically changes from a gaussian fall-off to a power-law reduction. In the limit of large Q^2 and conformal symmetry ($m = 0$), we find that $F_\pi^{s=1/2}(Q^2) \propto 1/Q^4$ for the spinor quark ($s = 1/2$) case but $F_\pi^{s=0}(Q^2) \propto 1/Q^2$ for the scalar quark ($s = 0$) case, i.e. the form factor with the Melosh factor being turned off in Eq. (3.1).

We find numerically that our $F_\pi^{s=0}(Q^2)$ is equivalent to the soft-wall AdS/QCD result [16] in the large Q^2 and conformal symmetry limit where the unconfined bulk-to-boundary propagator can be used, i.e. $F^{\mathrm{AdS/QCD}}_{(u.c.)}(Q^2) = \int_0^1 dx \exp[-(1-x)Q^2/4\kappa^2 x]$ (see Eq. (E.8) in [16]), where the subscript (u.c.) denotes the result of the unconfined current decoupled from the dilaton field. The

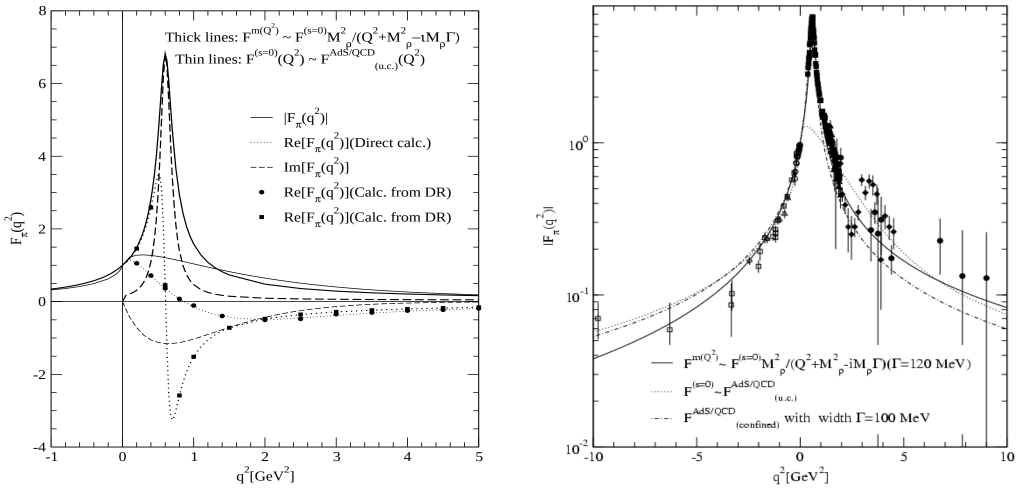

Figure 1: Left panel: Space- and timelike pion form factor obtained from $F_\pi^{m(Q^2)}(Q^2)$ (thick lines) and $F_\pi^{s=0}(Q^2)$ GeV (thin lines) compared with the results obtained from the dispersion relation(black data). Right panel: Space- and timelike pion form factor obtained from $F_\pi^{m(Q^2)}(Q^2)$ (solid line), $F_\pi^{s=0}(Q^2)$ GeV (dotted line), and $F^{\mathrm{AdS/QCD}}_{(confined)}(Q^2)$ (dot-dashed line), respectively.

pion form factor $F^{\mathrm{AdS/QCD}}_{(u.c.)}(Q^2)$ respecting the conformal symmetry shows the power-law behavior of $F_\pi(Q^2) \to 4\kappa^2/Q^2$ at large $Q^2(\gg \kappa^2)$. We note that the authors in [16] also derived the pion form factor in the presence of a dilaton field in AdS space and presented the analytic solution of the modified wave equation for the confined bulk-to-boundary propagator. This corresponds to the well-known vector dominance model (VDM) with the leading ρ resonance, i.e. $F^{\mathrm{AdS/QCD}}_{(confined)}(Q^2) = 4\kappa^2/(4\kappa^2+Q^2)$. Considering both spin and mass evolution effects in our LFQM analysis, we find that Eq. (3.1) with $m = m(Q^2)$ is well approximated by the following analytic form $F_\pi^{m(Q^2)}(Q^2) \simeq M_\rho^2 F_\pi^{s=0}(Q^2)/(Q^2+\mathscr{M}_\rho^2)$ up to intermediate spacelike momentum transfer region, where M_ρ is the physical mass of the ρ meson. We should note in the calculation of the timelike pion form factor that M_ρ^2 is replaced by $\mathscr{M}_\rho^2 = M_\rho^2 - iM_\rho\Gamma(q^2)$ in the denominator where $M_\rho = 776$ MeV and $\Gamma = 120$ MeV to compare with the timelike pion form factor data near the ρ peak.

In the left panel of Fig. 1, we show the pion form factor for both space- and timelike region obtained from $F_\pi^{m(Q^2)}(Q^2)$ (thick lines) and $F_\pi^{s=0}(Q^2)$ (thin lines), respectively. The solid, dotted, and dashed lines represent $|F_\pi(q^2)|$, $\mathrm{Re}[F_\pi(q^2)]$, and $\mathrm{Im}[F_\pi(q^2)]$, respectively. The black circles and squares are the results of $\mathrm{Re}[F_\pi^{s=0}(q^2)]$ and $\mathrm{Re}[F_\pi^{m(q^2)}(q^2)]$ obtained from the dispersion relation. This shows that our direct calculations are in an excellent agreement with the solutions of the dispersion relation. Although $F_\pi^{s=0}(Q^2)$ in timelike region produces a ρ meson-type peak near $q^2 \sim M_\rho^2$, it does not yield all the features of the vector meson dominance phenomena as $F_\pi^{m(Q^2)}(Q^2)$ does. This indicates that the spin and mass evolution effects are crucial in generating the more realistic features of the vector meson dominance phenomena. In the right panel of Fig. 1, we show the pion form factor for both space- and timelike region obtained from $F_\pi^{m(Q^2)}(Q^2)$ (solid line), $F_\pi^{s=0}(Q^2)$ GeV (dotted line), and $F^{\mathrm{AdS/QCD}}_{(confined)}(Q^2)$ [16] (dot-dashed line), respectively. Our $F_\pi^{m(Q^2)}(Q^2)$ and $F^{\mathrm{AdS/QCD}}_{(confined)}(Q^2)$ exhibit more realistic ρ meson-type peak than $F_\pi^{s=0}(Q^2)$. Our

LFQM analysis indicates that the difference between $F_\pi^{m(Q^2)}(Q^2)$ and $F_\pi^{s=0}(Q^2)$ is due to the spin (i.e. Melosh factor) and dynamical mass evolution effects of the constituent quark and anti-quark inside the pion. Our result may also be compared to the difference between $F^{\rm AdS/QCD}_{(confined)}(Q^2)$ and $F^{\rm AdS/QCD}_{(u.c.)}(Q^2)$, which is due to the effect of the dilaton field in AdS space [16].

4. Summary and Conclusion

In this talk, we presented recent progress of our LFQM phenomenology. In particular, we developed the analysis of spectroscopy in scalar mesons and their hadronic decays. According to our LFQM analysis, the $f_0(1710)$ is composed mainly of the scalar glueball, while the $f_0(1370)$ and $f_0(1500)$ are dominantly $n\bar{n}$–$s\bar{s}$ mixtures. Our result is consistent with the chiral suppression of the scalar glueball decay to a pair of quark and antiquark discussed by Chanowitz [14]. We also discussed the dispersion relation for the timelike pion form factor and our LFQM support on the recent findings from the AdS/QCD correspondence. In many respects, our LFQM provides a unified framework to analyze various experimental measurements for the hadron phenomenology.

References

[1] K. Hagiwara *et al.*, *Phys. Rev. D* **66** (2002) 010001 .

[2] J. Weinstein and N. Isgur, *Phys. Rev. Let.* **48** (1982) 659 ; *Phys. Rev. D* **41** (1990) 2236 ; S. Godfrey and N. Isgur, *Phys. Rev. D* **32** (1985) 189 ; R. Kokoski and N. Isgur, *Phy. Rev. D* **35** (1987) 907 .

[3] C. Amsler and F. E. Close, *Phys. Rev. D* **53** (1996) 295 .

[4] R. L. Jaffe, *Phys. Rev. D* **15** (1977) 267 ; *ibid.* **15** (1977) 281; **17** (1978) 1444.

[5] S. J. Brodsky and Guy F. de Teramond, *Phys. Rev. Lett.* **96** (2006) 201601 [hep-ph/0602252].

[6] H.-M. Choi and C.-R. Ji, *Phys. Rev. D* **74** (2006) 093010 [hep-ph/0608148].

[7] K. Abe *et al.*(Belle Collaboration), *Phys. Rev. Lett.* **89** (2002) 142001 [hep-ex/0205104]; *Phys. Rev. D* **70** (2004) 071102 [hep-ex/0407009]; B. Aubert *et al.*(Babar Collaboration), *Phys. Rev. D* **72** (2005) 031101 [hep-ex/0506062].

[8] H.-M. Choi and C.-R.Ji, in this conference proceedings, Pos(LC2008)016.

[9] H.-M. Choi and C.-R. Ji, *Phys. Rev. D* **59** (1999) 074015 [hep-ph/9711450]; *Phys. Lett. B* **460** (1999) 461 [hep-ph/9903496].

[10] M. A. DeWitt, H.-M. Choi and C. R. Ji, *Phys. Rev. D* **68** (2003) 054026 [hep-ph/0306060].

[11] S. Godfrey and N. Isgur, *Phys. Rev. D* **32** (1985) 189 .

[12] Martin DeWitt, *The Spectrum and Decays of Scalar Mesons in the Light–Front Quark Model*, Ph.D. Thesis, North Carolina State University (2008).

[13] J. Sexton and A. Vaccarino and D. Weingarten *Phys. Rev. Lett.* **75** (1995) 4563 .

[14] M. Chanowitz, *Phys. Rev. Lett.* **95** (2005) 172001 .

[15] S.J. Brodsky, *Eur. Phys. J. A* **31** (2007) 638 [hep-ph/0610115].

[16] S. J. Brodsky and Guy F. de Teramond, *Phys. Rev. D* **77** (2008) 056007 [arXiv:0707.3859 [hep-ph]].